Chinese Chemical Letters 35 (2024) 109419

Contents lists available at ScienceDirect

Chinese Chemical Letters

journal homepage: www.elsevier.com/locate/cclet

Direct detection of C9orf72 hexanucleotide repeat expansions by nanopore biosensor

Xinqiong Li[a,1], Guocheng Rao[b,1], Xi Peng[c], Chan Yang[a], Yanjing Zhang[a], Yan Tian[d], Xianghui Fu[d,*], Jia Geng[e,f,*]

[a] State Key Laboratory of Biotherapy and Cancer Center, West China Hospital, Sichuan University and Collaborative Innovation Center of Biotherapy, Chengdu 610041, China
[b] Division of Endocrinology and Metabolism, West China School of Medicine/West China Hospital, Sichuan University, Chengdu 610041, China
[c] Department of Endocrinology and Metabolism, Affiliated Hospital of North Sichuan Medical College, North Sichuan Medical College, Nanchong 637000, China
[d] Division of Endocrinology and Metabolism, National Clinical Research Center for Geriatrics, State Key Laboratory of Biotherapy and Cancer Center, West China Hospital, Sichuan University and Collaborative Innovation Center of Biotherapy, Chengdu 610041, China
[e] Department of Laboratory Medicine, State Key Laboratory of Biotherapy, Med-X Center for Manufacturing, West China Hospital, Sichuan University and Collaborative Innovation Center, Chengdu 610041, China
[f] Tianfu Jincheng Laboratory, City of Future Medicine, Chengdu 641400, China

ARTICLE INFO

Article history:
Received 8 November 2023
Revised 14 December 2023
Accepted 18 December 2023
Available online 22 December 2023

Keywords:
MspA nanopore
C9orf72 HRE
Detection
Biosensor
Catalytic hairpin assembly

ABSTRACT

Diagnostic C9orf72 hexanucleotide repeat expansions (C9-HRE) is essential for the early and accurate diagnosis of amyotrophic lateral sclerosis (ALS) and will provide support for the prognosis and gene therapy of ALS. In the present study, by combining catalytic hairpin assembly (CHA) with *Mycobacterium smegmatis* porin A (MspA) nanopore, a new nanopore-based strategy for the detection of C9-HRE was reported. Less than 30 repeats of C9-HRE could be detected *via* this method, and the results have the potential to help distinguish between patients and healthy individuals. Moreover, the method demonstrated its great specificity for C9-HRE by identifying other repeat expansions. Given the high selectivity, this approach had been successfully used to detect C9-HRE in cell and blood samples with high accuracy. This detection strategy is user-friendly and has a strong anti-interference ability, thus providing a powerful tool for clinical diagnosis.

A GGGGCC hexanucleotide repeat expansion (HRE) in the first intron of chromosome 9 open reading frame 72 (C9orf72) is the most prevalent genetic trigger for amyotrophic lateral sclerosis (ALS) and frontotemporal dementia (FTD) [1,2]. The HRE not only impacts RNA transcription and translation but also forms aggregates in cells, generating unstable RNA or protein that could lead to neuronal death. Around 5%–10% of patients with FTD or ALS and up to 30% of patients with both have the HRE reported [3,4]. Several studies have revealed that the length of HRE determines how pathogenic it is, however, it is unclear where to draw the boundary between normal and pathogenic alleles. Less than 30 repeats are often present in healthy persons, whereas hundreds to thousands of repeats are typically present in individuals with C9orf72-related illnesses [1,2,5]. The discovery of the C9orf72 HRE (C9-HRE) can be employed in clinical diagnosis and genetic counseling for ALS and FTD [3,6–8]. It not only aids in the distinction between genetic variations and other factors linked to these two diseases but also serves as a foundation for the creation of therapeutic approaches for both disorders.

To accurately determine and estimate the length of the C9-HRE, the southern blot as the gold standard can be performed. However, the drawback of the southern blot is that it is challenging and time-consuming [9]. In addition, polymerase chain reaction (PCR)-based assays are frequently used to determine C9-HRE length, but sequence variants (*e.g.*, deletions and insertions) reduce the accuracy of those methods [5,10,11]. In current studies, short- and long-read sequencing techniques are invented to detect and size the C9-HRE [12–14]. Although these techniques achieve excellent results, reconstructing expansions using short-read sequencing methods is still challenging, and long-read sequencing usually has a fairly low number of reads bridging expansions. Hence, there is an urgent requirement for a C9-HRE assay that is straightforward, quick, and

* Corresponding authors.
E-mail addresses: xfu@scu.edu.cn (X. Fu), geng.jia@scu.edu.cn (J. Geng).
[1] These authors contributed equally to this work.

https://doi.org/10.1016/j.cclet.2023.109419
1001-8417/

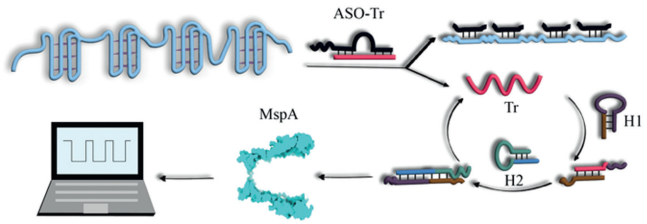

Fig. 1. Schematics illustration of the detection of C9orf72 HRE on the basis of target-triggered catalytic hairpin assembly using the nanopore sensor.

highly accurate for the early detection and treatment of C9orf72-related diseases.

Biosensors, which are devices for detecting and measuring certain organisms or chemicals, have been utilized in a variety of applications [15–18]. Nanopore sensing is a quick method that can identify single molecules in real-time. The target molecule can electrophoretically pass through the nanopore under an applied voltage after a membrane protein that forms nanopores has been reconstituted in a lipid bilayer. Due to it can analyze single molecules, nanopore sensing has a wide variety of applications, including DNA sequencing [19,20], protein analysis [21–24], and detection of small molecules [25–29]. There has recently been a surge in interest in the use of nanopore sensors to quantify biomarkers in clinical samples [30–35]. Currently, there are few reports of nanopore sensing technologies being used to detect ALS and FTD biomarkers [13].

In this study, we focus on the use of nanopore sensors for the detection of C9-HRE. More specifically, longer-length C9-HRE would trigger the release of more ssDNA, which stimulates catalytic hairpin assembly (CHA) to produce dsDNA, which could then result in current blockage in the *Mycobacterium smegmatis* porin A (MspA) nanopore. This approach allows accurate quantification of C9-HRE, enabling new concepts and procedures for the clinical diagnosis and treatment of ALS and FTD.

The principle of C9-HRE detection using the target-triggered CHA amplification strategy is presented in Fig. 1. This system comprised a double chain structure ASO-Tr, and two unlabeled hairpin probes designated Harpin 1 (H1) and Harpin 2 (H2). Double chain structure ASO-Tr contained antisense oligonucleotides (ASO) as the aptamer and trigger (Tr). In the absence of C9-HRE, the combination of Tr and ASO prevented CHA from being triggered, and no resulting structure was detected with MspA nanopores. ASO could easily bind C9-HRE in the presence of C9-HRE, forming an aptamer- HRE complex, and the trigger was released. Then, H1 was opened *via* complementary attachment to the 3′ of the Tr strand, exposing the 3′ of the H1. The 3′ of the H1 hybridized with H2 to form a Tr-H1-H2 complex. As the Tr-H1-H2 complex was inherently less stable than H1-H2, Tr could be replaced by H2 through spontaneous disassembly. The Tr that was displaced bound to a new H1 and triggered a new round of the CHA process. Each copy of the target C9-HRE could initiate numerous assembly processes through the CHA cycle, resulting in a significant amount of H1-H2 duplexes. This increased the effectiveness of target conversion and amplification. The H1-H2 duplex was detected *via* a MspA nanopore.

For verification of the successful formation of CHA, the reaction was analyzed by native polyacrylamide gel electrophoresis (PAGE). PAGE images were presented in Fig. S1 (Supporting information). As shown in Fig. S1A, lanes 1–5 correspond to H2, H1, Tr, H1-H2, and ASO-Tr-H1-H2, respectively. In particular, there were two additional bands in lane 6 compared to lane 5. To further confirm the two bands in lane 6, single-stranded H1-L and H2-L were annealed and then analyzed by native PAGE. As shown in Fig. S1B, the H1-L-H2-L hybrid band (land 5) posed at the highest position compared to hairpin DNA and the combinations of two DNA, indicated that the upper band in land 4 was H1-H2 hybrid band and the lower band in land 4 was Target-ASO (T-ASO). The result demonstrated that when T was present, the CHA reaction could be triggered to form H1-H2 hybridization structure. Since the molecular weight of H1-H2 hybridization structure was larger than both H1-H2 and T-ASO, it had the slowest migration rate in PAGE. Furthermore, a weak band was observed in land 5, at the same position as the H2, which may represent the formation of other secondary structures by single-stranded DNA. Collectively, these results confirmed the rational design of DNA sequences that facilitated CHA reaction and enabled the detection of the target sequence.

To illustrate the feasibility of employing a nanopore as a single-molecule stochastic sensing element for C9-HRE detection, the translocation of ASO-Tr, H1, H2, and H1-H2 hybridization complexes in the nanopore was first investigated at an applied potential bias of +120 mV. In line with our expectations, each of the three structures gave rise to unique translocation events that were easily distinguishable from one another (Fig. 2). In this report, the open pore current was defined as I_o, the residual current was I, and the event dwell time was t. The percentage blockade was defined as $(I_o - I)/I_o$. The event histogram data was analyzed using a Gaussian distribution. In the present study, the characteristic ionic current blockades elicited by both ASO-Tr and hairpin (H1 and H2) were observed, which incorporated two residual current levels: a shallow blockade (level 1) and a deeper one (level 2) (Figs. 2A–C). The percentage blockade for ASO-Tr, H1 and H2 at current level 1 were 0.43 ± 0.01, 0.33 ± 0.01 and 0.35 ± 0.01, respectively. For current level 2, ASO-Tr, H1 and H2 showed 0.82 ± 0.01, 0.78 ± 0.01 and 0.79 ± 0.04, respectively. The dwell times at level 1 for ASO-Tr, H1, and H2 were 2.82 ± 0.05 ms, 3.52 ± 0.10 ms and 2.87 ± 0.08 ms, respectively. Meanwhile, the dwell times at level 2 were 0.54 ± 0.03 ms, 0.55 ± 0.07 ms, and 0.18 ± 0.02 ms for ASO-Tr, H1, and H2, respectively. As mentioned in our previous work, the shallow blockage of the hairpin was caused by its collision with the vestibule of the MspA nanopore, whereas the deeper blockage was brought about by efficient translocation [36]. The voltage-dependent experiment also supported the conclusions (Figs. S2–S4 in Supporting information). Notably, the type of events and properties of ASO-Tr were consistent with the hairpin structure. Most likely, ASO-Tr contained a loop structure that could collide with the MspA nanopore vestibule, just as the previously reported hairpin structure interacted with MspA [36]. Similar to other dsDNA translocate through the nanopore, only one type event was observed for H1-H2 hybridization complexes translocating through the MspA nanopore, with the blockade rate at 0.84 ± 0.002 and the dwell time at 3.32 ± 0.05 ms (Fig. 2D and Fig. S5 in Supporting information). Given that the translocation events are voltage- and concentration-dependent [37], the current events of H1-H2 hybridization complexes were further characterized by voltage- and concentration-dependence in this investigation. The results demonstrated that the dwell time exhibited strong voltage-dependent (Fig. 2F). Simultaneously, the translocation events frequency increased linearly with increasing H1-H2 hybridization complexes concentration (Fig. 2E). The above results confirmed that target-triggered CHA amplification strategy could be used to detect C9-HRE.

Considering that C9-HRE detection could be achieved using nanopores, we next applied this strategy to different C9-HRE length detection. Because the ASO sequence was perfectly complementary to the C9-HRE, the frequency of the H1-H2 hybridization complex events increased as the repeat units increased. As shown in Fig. 3A, there was a dividing line at 15 repeats. For repeat lengths below 15, the event frequency of H1-H2 hybridization increased with the number of repeat units, whereas for repeat lengths exceeding 15, the event frequency decreased. To investi-

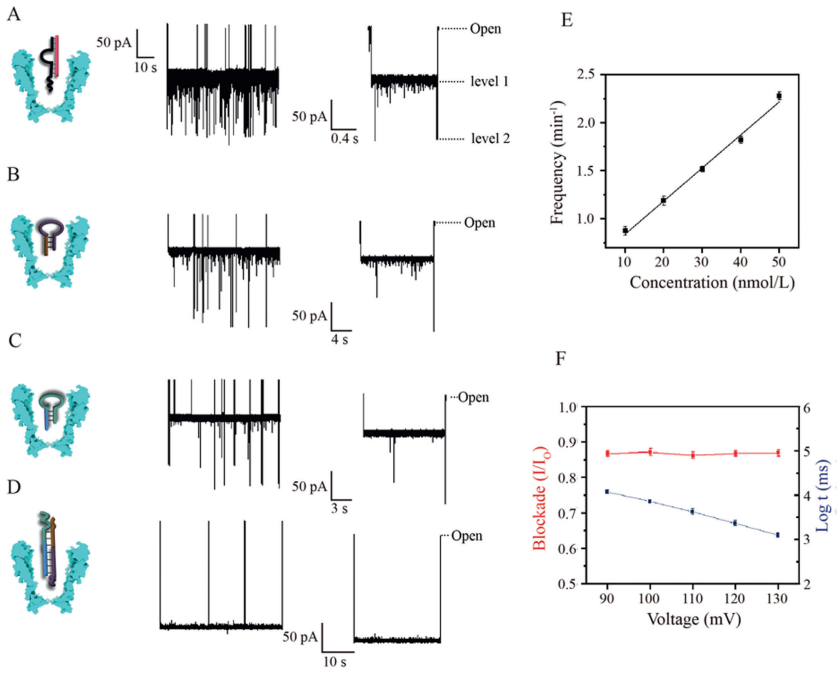

Fig. 2. Characterization of DNA structures using a MspA nanopore. The ASO-Tr (A), H1 (B), H2 (C) and H1–H2 hybridization (D) structures translocation through the nanopore. Left: illustration of DNA structures translocating through a nanopore. Middle: the typical current and time traces of DNA structures at +120 mV. Right: the zoomed-in view of the current blockade segments of the typical events. The typical signals of other DNA structures show a shallow blockade and a deeper one, in contrast to the typical signals of H1–H2 hybridization complexes, which have a deep blockade and long duration. (E) The event frequency *versus* H1–H2 hybridization concentration. (F) Characteristic blockade (shown in red) and dwell time (shown in blue) of H1-H2 hybridization as a function of the applied voltage.

gate this, it is possible that the G-quadruplex structure (G4) was formed due to an increase in repeat units, and that ASO unfolding the G4 structure is G-rich sequence dependent [38], resulting in less H1-H2 hybridization complexes formation. Using this strategy, it is possible to distinguish patients who carry the C9-HRE from healthy individuals. While the event frequency is greater than 0.5, then the repeat length is lower than 30, indicating that the individual is healthy.

To investigate the selectivity of the developed nanopore sensing strategy, other repeat expansion sequences that may play a role in disease were investigated. The products of C9-HRE and other repeat extension sequences were first analyzed through native PAGE. We found that, compared to the control and other lanes, the H1-H2 hybrid band posed at the highest position only in the absence of C9-HRE (Fig. S6 in Supporting information). Next, all products were also examined using nanopore sensing. In contrast, the event frequency of other repeat extension sequences was significantly lower than that of C9-HRE which was approximately the same as the control (Fig. 3B). The above results demonstrated that other repeat extension sequences failed to trigger the CHA reaction and this strategy was able to specifically detect C9-HRE. The complete complementary pairing of ASO and C9-HRE enhanced the specificity of this strategy.

As C9orf72 is expressed in cells, its detection may be impacted by other nucleic acids or small molecules in the cells. Then, we combined HEK293T cells with C9-HRE and collected DNA and RNA for analysis to evaluate this strategy's anti-interference ability. As shown in Fig. 4, there was no significant difference in the event frequency of the H1–H2 hybridization complexes, whether extracted together or added to C9-HRE after extraction, which was much higher than that of the control. To further evaluate the applicability of the developed method to real biological samples, the

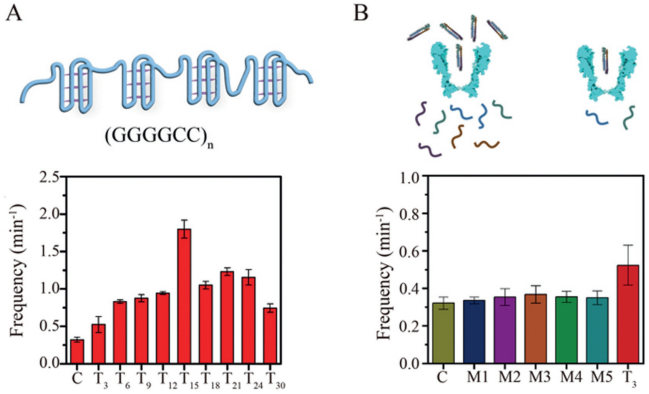

Fig. 3. Detection of the C9orf72 hexanucleotide repeat expansion using a MspA nanopore. (A) Detection of different lengths of C9orf72 hexanucleotide repeat expansion. (B) Selectively detection of C9orf72 hexanucleotide repeat expansion. Data represent mean ± standard deviation (SD) ($n = 3$).

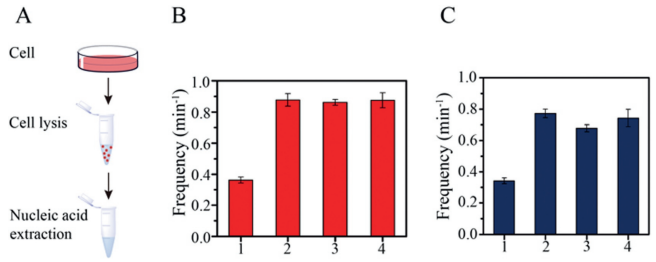

Fig. 4. Detection C9orf72 hexanucleotide repeat expansion in HEK 293T cells. Both DNA and RNA were observed and analyzed using a MspA nanopore. (A) Schematic representation of the extraction of nucleic acid from the cell sample. (B) Lane 1: Cellular DNA; lane 2: Extrinsic T_9 DNA added to extracted cellular DNA; lane 3: Extrinsic T_9 DNA added to cell suspension; lane 4: Extrinsic T_9 DNA. (C) Lane 1: Cellular RNA; lane 2: Extrinsic T_{30} RNA added to extracted cellular RNA; lane 3: Extrinsic T_{30} RNA added to cell suspension; lane 4: Extrinsic T_{30} RNA. Data represent mean ± SD ($n = 3$).

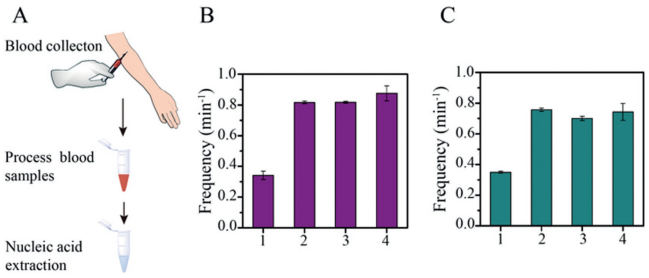

Fig. 5. Detection C9orf72 hexanucleotide repeat expansion in blood from healthy persons. Both DNA and RNA were observed and analyzed using a MspA nanopore. (A) Schematic representation of the extraction of nucleic acid from the blood sample. (B) lane 1: Blood DNA; lane 2: Extrinsic T_9 DNA added to extracted blood DNA; lane 3: Extrinsic T_9 DNA added to blood; lane 4: Extrinsic T_9 DNA. (C) Lane 1: Blood RNA; lane 2: Extrinsic T_{30} RNA added to extracted blood RNA; lane 3: Extrinsic T_{30} RNA added to blood; lane 4: Extrinsic T_{30} RNA. Data represent mean ± SD ($n = 3$).

strategy was used to detect healthy volunteer blood samples with C9-HRE. Nucleic acid extraction from human blood samples was carried out in the same method as cells. It was found that the event frequency of each group of H1-H2 hybridization complexes was consistent with the cells for both RNA and DNA samples (Fig. 5). These results demonstrated the superior ability of the strategy to discriminate C9-HRE from interfering analytes and its potential for use in clinical applications.

In summary, this work exhibits a strategy that successfully detects C9-HRE through nanopores using a target-triggered CHA reaction. Unlike PCR methods that cannot quantify repeat number [39], this study utilizes ASO which is fully complementary to C9-HRE, allowing for quantitative analysis of C9-HRE length. It is worth noting that the ability of the developed method to specifically identify C9-HRE from the analytes is also attributable to the full complementarity between ASO and HRE. Meanwhile, the developed method was applied to the detection of complex samples with satisfactory results. In conclusion, the developed method possesses the advantages of anti-interference ability, high specificity, and simplicity, and has great potential for use in the detection of clinical samples. Furthermore, since other repeat expansion sequences can also lead to disease, the principle of the strategy in this study can be used for other disease detection by designing corresponding ASO.

Ethical statement

All of the human subject experiments were approved by the West China Hospital, Sichuan University Medical Ethics Committee and conformed to the principles of the Declaration of Helsinki.

Declaration of competing interest

The authors declare that they have no known competing financial interests or personal relationships that could have appeared to influence the work reported in this paper.

Acknowledgments

This work was supported by a grant from the National Key Research and Development Program of China (No. 2022YFB3205600); National Natural Science Foundation of China (No. 82004341); China Postdoctoral Science Foundation (No. 2022M712286); Sichuan Science and Technology Program (No. 2020JDTD0022); Sichuan Administration of Traditional Chinese Medicine (No. 2023MS078); Sichuan University Postdoctoral Interdisciplinary Innovation Fund (No. JCXK2225).

Supplementary materials

Supplementary material associated to this article can be found, in the online version, at doi:10.1016/j.cclet.2023.109419.

References

[1] M. DeJesus-Hernandez, I.R. Mackenzie, B.F. Boeve, et al., Neuron 72 (2011) 245–256.
[2] A.E. Renton, E. Majounie, A. Waite, et al., Neuron 72 (2011) 257–268.
[3] E. Majounie, A.E. Renton, K. Mok, et al., Lancet Neurol. 11 (2012) 323–330.
[4] C. Marogianni, D. Rikos, A. Provatas, et al., Neurobiol. Aging 84 (2019) 238.e25–238.e34.
[5] J. van der Zee, I. Gijselinck, L. Dillen, et al., Hum. Mutat. 34 (2013) 363–373.
[6] J. Roggenbuck, J.C. Fong, Clin. Lab. Med. 40 (2020) 271–287.
[7] S. Ducharme, A. Dols, R. Laforce, et al., Brain 143 (2020) 1632–1650.
[8] A. Crook, A. McEwen, J.A. Fifita, et al., Amyotroph. Lateral Scler. Front. Degener. 20 (2019) 310–316.
[9] M. van Blitterswijk, M. DeJesus-Hernandez, E. Niemantsverdriet, et al., Lancet Neurol 12 (2013) 978–988.
[10] A. Nordin, C. Akimoto, A. Wuolikainen, et al., Amyotroph. Lateral Scler. Front. Degener. 18 (2017) 256–264.
[11] H. Hanson, A.F. Brady, G. Crawford, et al., J. Med. Genet. 58 (2021) 135–139.
[12] E. Dolzhenko, J.J.F.A. van Vugt, R.J. Shaw, et al., Genome Res. 27 (2017) 1895–1903.
[13] M.T.W. Ebbert, S.L. Farrugia, J.P. Sens, et al., Mol. Neurodegener. 13 (2018) 46.
[14] P. Giesselmann, B. Brändl, E. Raimondeau, et al., Nat. Biotechnol. 37 (2019) 1478–1481.
[15] X. Lv, L. Zhu, Y. Rong, et al., Biosens. Bioelectron. 214 (2022) 114522.
[16] P. Zhu, S. Li, S. Zhou, et al., Chem. Eng. J. 420 (2021) 127559.
[17] L. Zhu, X. Lv, H. Yu, et al., Anal. Chem. 94 (2022) 8327–8334.
[18] Y. Huang, Y. Lv, J. Geng, D. Xiao, C. Zhou, Chin. Chem. Lett. 31 (2020) 172–176.
[19] P.S. Krstic, V. Tabard-Cossa, G.V. Soni, et al., Nat. Biotechnol. 26 (2008) 1146–1153.
[20] Y.L. Ying, Z.L. Hu, S. Zhang, et al., Nat. Nanotechnol. 17 (2022) 1136–1146.
[21] J. Jiang, M.Y. Li, X.Y. Wu, et al., Nat. Chem. 15 (2023) 578–586.
[22] X. Zhang, N.S. Galenkamp, N.J. van der Heide, et al., ACS Nano 17 (2023) 9167–9177.
[23] L. Restrepo-Pérez, C. Joo, C. Dekker, Nat. Nanotechnol. 13 (2018) 786–796.
[24] K. Xin, Z. Hu, S. Liu, et al., Angew. Chem. Int. Ed. 61 (2022) e202209970.
[25] M.Y. Li, Y.Q. Wang, Y.L. Ying, Y.T. Long, Chem. Sci. 10 (2019) 10400–10404.
[26] C. Zhao, K. Li, X. Mou, et al., Biosens. Bioelectron. 200 (2022) 113894.
[27] K. Sun, P. Chen, S. Yan, et al., ACS Appl. Mater. Interfaces 13 (2021) 21030–21039.
[28] X. Li, P. Zhang, L. Dou, et al., ACS Sens. 5 (2020) 2359–2366.
[29] Q. Zhang, Y. Cheng, P. Cao, Z. Gu, Chin. Chem. Lett. 30 (2019) 1607–1617.
[30] J.Y.Y. Sze, A.P. Ivanov, A.E.G. Cass, J.B. Edel, Nat. Commun. 8 (2017) 1552.
[31] S. Cai, T. Pataillot-Meakin, A. Shibakawa, et al., Nat. Commun. 12 (2021) 3515.
[32] N. Burck, T. Gilboa, A. Gadi, et al., Clin. Chem. 67 (2021) 753–762.
[33] K. Chuah, Y. Wu, S.R.C. Vivekchand, et al., Nat. Commun. 10 (2019) 2109.
[34] Y. Wu, Y. Yao, S. Cheong, R.D. Tilley, J.J. Gooding, Chem. Sci. 11 (2020) 12570–12579.
[35] R. Ren, M. Sun, P. Goel, et al., Adv. Mater. 33 (2021) 2103067.
[36] X. Li, G. Song, L. Dou, et al., Nanoscale 13 (2021) 11827–11835.
[37] M. Wanunu, J. Sutin, B. McNally, A. Chow, A. Meller, Biophys. J. 95 (2008) 4716–4725.
[38] T.Y. Tseng, S.Y. Liu, C.L. Wang, T.C. Chang, Molecules 25 (2020) 4083.
[39] V.L. Buchman, J. Cooper-Knock, N. Connor-Robson, et al., Mol. Neurodegener. 8 (2013) 12.